Adiabatic matching of a nonuniform intense charged-particle beam into the focusing channel

Yuri K. Batygin
The Institute of Physical and Chemical Research (RIKEN), Hirosawa, 2-1, Wako-shi, Saitama, 351-01, Japan
(Received 23 February 1996; revised manuscript received 9 May 1996)

Adiabatic matching of a bright beam into a transport focusing channel, while avoiding beam halo formation, is considered. Gradual changes in nonlinear focusing fields result in the modification of an initially nonlinear beam distribution into a distribution matched with the linear focusing channel. A plasma lens with a specific distribution of particles along the channel provides an ideal way to create an appropriate nonlinear focusing field. Another method employs an alternating-gradient focusing quadrupole structure with a multipole component of sixth order (duodecapole component). In this case, the initial matched beam profile has to be close to square instead of the conventional circular beam cross section. Analytical results are illustrated by simulations using the particle-in-cell method. [S1063-651X(96)05111-2]

PACS number(s): 07.77.−n, 29.27.Eg, 41.75.−i, 52.25.Wz

I. INTRODUCTION

Experiments that use intense particle beams exhibit strong emittance growth and beam halo formation in the linear focusing channel due to a mismatch between the beam profile and the focusing field. This phenomenon limits beam brightness and results in particle loss. In the next generation of intense particle accelerators for heavy ion fusion [1] and nuclear waste transmutation [2] beam halo will have to be suppressed. Recently [3,4], it was shown that the emittance of a high brightness beam can be conserved in a highly nonlinear focusing field. Such a focusing field must be a linear function of the radius near the axis and decay nonlinearly further from the axis. An ideal method of creating this potential distribution is to use a plasma lens with a specific distribution of particles with opposite charge. Another method utilizes an alternating-gradient quadrupole structure with a higher-order (duodecapole) field component, where approximate matched conditions for the beam can be obtained.

Most existing beam transport channels are based on focusing elements dominated by linear fields produced by quadrupoles, solenoids, and electrostatic axial-symmetric lenses. An adiabatic variation of a nonlinear focusing field can be expected to provide a gradual transformation of an initially nonlinear beam distribution into a distribution matched to the linear focusing channel. In this case, it is only necessary to create a complicated nonlinear focusing for a short distance in an adiabatic transformer. To match a beam with an arbitrary distribution function into the linear focusing channel, two problems must be solved: to create an appropriate focusing potential distribution and conserve the given beam distribution function and to provide an adiabatic transformation into the potential of a conventional focusing structure with a linear focusing field.

This paper studies the behavior of a space-charge-dominated beam in a uniform focusing channel and in an alternating-gradient structure with a small value of phase advance per period. In such systems, the envelopes of the matched beams are nearly constant. This makes it possible to consider a z-independent process and treat the problem analytically.

II. MATCHING OF A BEAM INTO THE UNIFORM FOCUSING CHANNEL

Self-consistent matched conditions for a beam with an arbitrary distribution function in a uniform focusing channel have been obtained from two principles: Vlasov's equation for a time-independent distribution function and Poisson's equation for the space-charge potential of the beam [3,4]. A realistic beam distribution is characterized by a high concentration of particles near the axis and declining particle density towards the periphery of the beam. Let us consider a beam of particles with a parabolic distribution function, which is similar to experimentally observed beam distributions. In this distribution, the phase-space density of particles monotonically decreases from the center of the beam until reaching the boundary of a four-dimensional hypervolume:

$$f=\frac{3}{2\pi^2}\frac{I}{\beta q m^2 c^3 \varepsilon^2}\left(1-\frac{x^2+y^2}{2R^2}-\frac{p_x^2+p_y^2}{2p_0^2}\right), \qquad (1)$$

where I is the beam current, β is the longitudinal particle velocity, q is the charge, m is the mass of particle, $R=2\sqrt{\langle x^2\rangle}$ is the beam envelope, $p_0=2\sqrt{\langle p_x^2\rangle}$ is the double root mean square (rms) beam size in phase space, and ε is the normalized rms beam emittance

$$\varepsilon=\frac{4}{mc}\sqrt{\langle x^2\rangle\langle p_x^2\rangle-\langle x p_x\rangle^2}=R\frac{p_0}{mc}. \qquad (2)$$

The space charge density ρ_b and space charge potential of the beam U_b are defined by the expressions

$$\rho_b=\frac{3I}{2\pi c\beta R^2}\left(1-\frac{r^2}{2R^2}\right)^2, \qquad (3)$$

$$U_b=-\frac{3}{2}\frac{mc^2}{q}\frac{I}{I_c\beta}\left(\frac{r^2}{R^2}-\frac{r^4}{4R^4}+\frac{r^6}{36R^6}\right), \qquad (4)$$

where $I_c=4\pi\varepsilon_0 mc^3/q=(A/Z)3.13\times10^7$ A is the characteristic value of beam current. Substitution of the distribution (1) into Vlasov's equation for a time-independent distribution function gives

TABLE I. Beam emittance growth in a uniform focusing channel.

Curve	Beam distribution and focusing channel	Initial emittance (π cm mrad)	Final emittance (π cm mrad)
1*a*	parabolic beam in a linear focusing field	0.12	0.14
1*b*	parabolic beam in a nonlinear adiabatic matcher	0.12	0.126
1*c*	KV beam in a linear focusing field	0.12	0.124

$$\frac{df}{dt}=\frac{\partial f}{\partial x}v_x+\frac{\partial f}{\partial y}v_y-q\left(\frac{\partial f}{\partial p_x}\frac{\partial U}{\partial x}+\frac{\partial f}{\partial p_y}\frac{\partial U}{\partial y}\right)=0, \quad (5)$$

leading to the expression for the total potential of the structure

$$U=\frac{mc^2}{q}\frac{\varepsilon^2}{R^4}\left(\frac{x^2+y^2}{2}\right)=\frac{1}{2}\frac{mc^2}{q}\frac{\varepsilon^2 r^2}{R^4}. \quad (6)$$

The potential $U=U_{\rm ext}+U_b$ is a combination of the potential of an external focusing field $U_{\rm ext}$ and the space charge potential U_b of the beam. Combining the solution of Vlasov's equation for total potential of the structure U and space charge potential of the beam U_b, the required potential to maintain a given distribution function can be found:

$$U_{\rm ext}=\frac{mc^2}{q}\left[\frac{r^2}{2R^2}\left(\frac{\varepsilon^2}{R^2}+\frac{3I}{I_c\beta}\right)+\frac{3I}{8I_c\beta}\left(-\frac{r^4}{R^4}+\frac{r^6}{9R^6}\right)\right]. \quad (7)$$

The potential (7) consists of a quadratic term r^2, describing the linear focusing, and two nonlinear terms, proportional to r^4 and r^6. The nonlinear terms compensate exactly for the corresponding nonlinear terms in the space charge potential of the beam, while the quadratic term, in combination with the corresponding quadratic term for the space charge potential, creates a total linear focusing, defined by the value of the beam emittance (2). This comes from the fact that the parabolic beam distribution (1) provides elliptical phase-space projections at phase planes $x-p_x$ and $y-p_y$ and the ellipse is conserved in a linear field. Therefore, the total field of the structure has to be a linear function of the radius, but the external focusing field appears as a nonlinear function of radius. The required potential for the focusing field (7) is substantially different from fields widely used in conventional transport channels.

III. ADIABATIC TRANSFORMATION OF A NONLINEAR BEAM DISTRIBUTION

Conservation of the beam distribution function requires the focusing field to be linear near the axis and become essentially nonlinear far from the axis. Conventional focusing structures employ quadrupole lenses and axial-symmetric lenses (both electrostatic and magnetostatic) where linear focusing components usually dominate. It is interesting to verify whether it is possible to transform an initially nonlinear distribution into a distribution matched with the linear focusing channel. Suppose the focusing field (7) provides perfect matching of the initial nonuniform beam and subsequent changes in the focusing field are done adiabatically. In this case the beam emittance is a constant of motion [5]

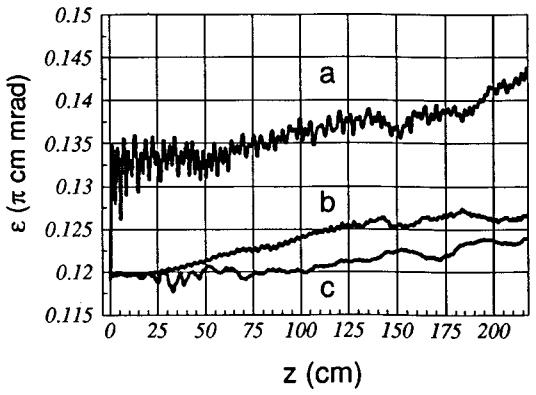

FIG. 1. rms beam emittance growth in a uniform focusing channel: (a) beam with a parabolic distribution in a linear field, (b) beam with a parabolic distribution in the matching section with a nonlinear field, and (c) KV beam in a linear field.

$$\varepsilon=\int dx\, dp_x=inv. \quad (8)$$

The restriction of an adiabatic change of parameters means that the system should change more slowly than the period of oscillation of the beam particles. The adiabatic invariant (8) is not conserved exactly during the field transformation [5], but one can expect that any change of the value of the invariant (beam emittance) will be small.

The final expected beam distribution is a distribution that is matched with a linear focusing structure. This class of matched beams was studied in detail in Refs. [6–10]. A general property of those solutions is that, with increasing beam current, the profile of the matched beam has to become increasingly flat, while the phase-space projection (beam emittance) has to become ever closer to rectangular.

To verify the possibility of adiabatic beam transformation, a self-consistent computer simulation using the particle-in-cell code BEAMPATH [11] for the proton beam with $I=2$ A, $R=0.15$ cm, $\varepsilon=0.12$ π cm mrad, and $\beta=0.01788$ was done. The beam was represented as a combination of 3×10^4 particles. Trajectories were calculated employing the leapfrog method [12] and the two-dimensional space charge potential of the beam was calculated for the instantaneous particle distribution at every time step with a fast Fourier transform on a spatial grid of 256×256.

The focusing field potential was gradually transformed from the field (7), required by nonlinear matched conditions, to the linear focusing field

$$U(r,z)=U_{\rm ext}(r)+[U_L(r)-U_{\rm ext}(r)]\frac{z}{L}, \quad (9)$$

where z is the longitudinal coordinate and L is the drift space of the matcher. The potential U_L was chosen as a potential that provides a matched condition for an equivalent

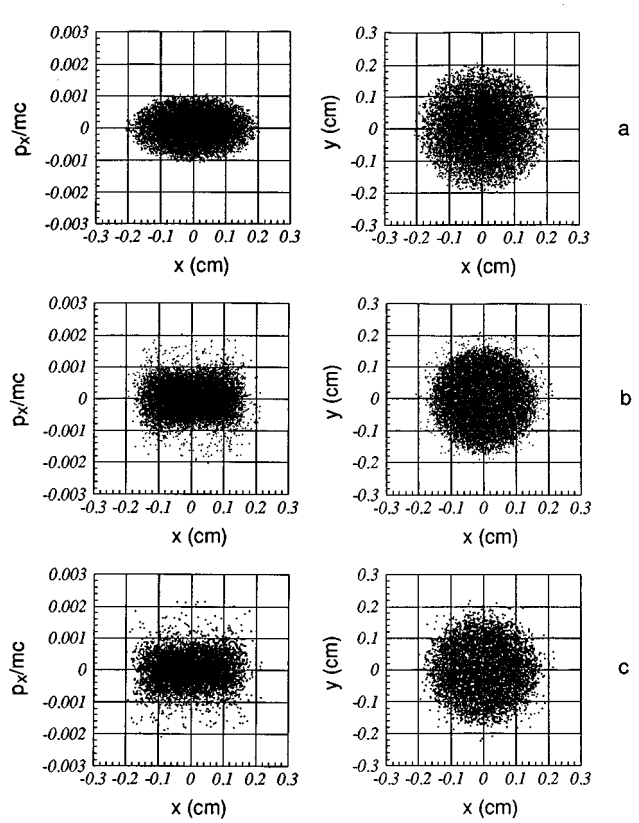

FIG. 2. Beam emittance growth in a uniform focusing channel with a linear focusing field: (a) $z=0$, (b) $z=114$ cm, and (c) $z=228$ cm.

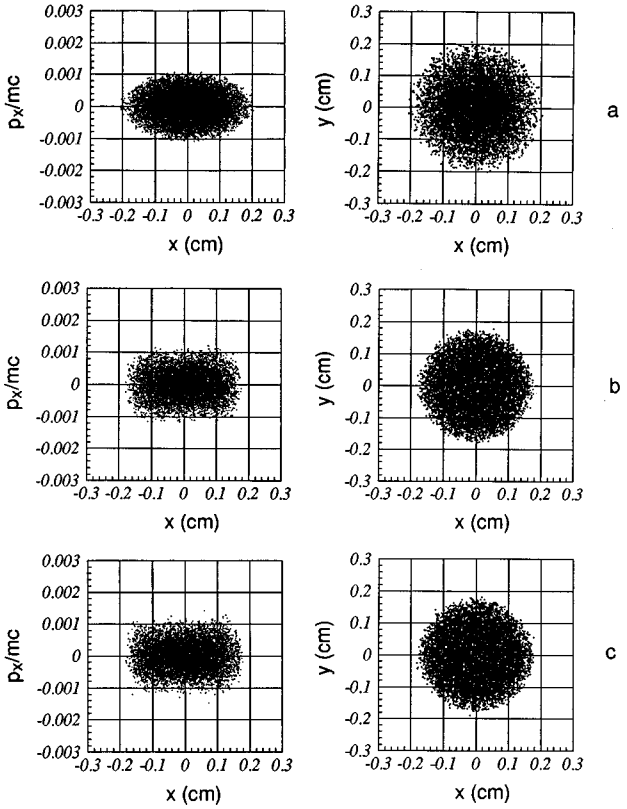

FIG. 3. Adiabatic matching of the beam in a uniform nonlinear matching section: (a) $z=0$, (b) $z=114$ cm, and (c) $z=228$ cm.

Kapchinsky-Vladimirsky (KV) [6] beam in a linear focusing channel, with the same rms beam emittance ε and rms beam envelope R:

$$U_L(r)=\frac{mc^2}{q}\left(\frac{\varepsilon^2}{2R^4}+\frac{I}{I_c\beta R^2}\right)r^2. \tag{10}$$

The distance $L=114$ cm was selected to allow five transverse oscillations of the particles along the matcher. After adiabatic transformation, the beam was transported 114 cm further in the linear focusing channel to check the result of adiabatic matching. For comparison, the beam dynamics in the pure linear focusing channel with a potential U_L for initial parabolic [Eq. (1)] and KV distributions were calculated. The results of simulation are presented in Table I and Figs. 1–3.

Calculations show that, in a pure linear focusing channel, a beam with a parabolic distribution experiences halo formation and emittance growth, while during adiabatic transformation in a nonlinear matching section, halo formation is avoided and emittance growth is substantially smaller. The beam emittance of a parabolic beam distribution in the linear focusing channel changed rapidly from the initial value 0.12 π cm mrad to become 0.135 π cm mrad during the first 1.28 cm of beam transport. The emittance growth rate $d\varepsilon/dz$ was 10^{-2} (π cm mrad)/cm [see Fig. 1(a)]. The same distribution in the nonlinear matcher exhibited almost constant emittance, with an emittance growth rate $d\varepsilon/dz=10^{-4}$ (π cm mrad)/cm, which is two orders of magnitude smaller [see Fig. 1(b)]. The phase-space projection of the beam in the matching section changed due to a variation in the focusing field and the final beam distribution is completely matched with the linear channel. This study shows that the nonuniform beam distribution can be transformed into a distribution that is matched with a linear focusing channel, using a relatively short adiabatic matching section with a nonlinear focusing field.

Figure 1(c) indicates the emittance growth of a KV beam due to numerical errors. An ideal KV distribution provides linear space charge forces, which, in combination with linear

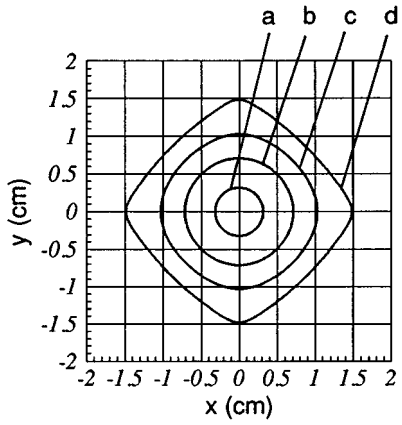

FIG. 4. Lines of equal values of the function $\Phi=r^2+2\zeta r^6(\cos2\varphi\cos6\varphi+\sin2\varphi\sin6\varphi)+\zeta^2r^{10}$ for $\zeta=-0.025$: (a) $\Phi=0.1$, (b) $\Phi=0.5$, (c) $\Phi=1.0$, and (d) $\Phi=1.7$.

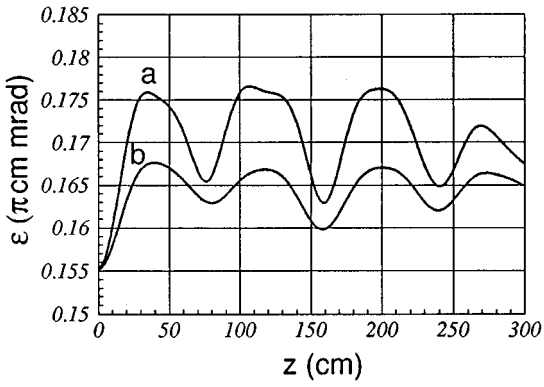

FIG. 5. rms beam emittance growth in a pure quadrupole alternating-gradient focusing channel with $G_2=40$ kV/cm^2: (a) circular beam and (b) square beam.

focusing forces, guarantee preservation of beam emittance. In a numerical experiment employing the particle-in-cell method, the space charge forces are not perfectly linear due to the finite number of modeling particles and mesh points required to solve the space-charge problem. This results in the nonconservation of beam emittance, which in this case is 3% after ten transverse oscillations for a high brightness beam with a phase-space density of 16.6 A/(π cm mrad). The proximity of the emittance growth curves for a KV beam in a linear focusing channel and a parabolic beam in a nonlinear matcher in Fig. 1 indicates that emittance growth in a nonlinear matcher is partly due to numerical errors and similar matching conditions for a KV beam in linear field are achieved.

The required nonlinear focusing field can be created by a graded distribution of oppositely charged particles along the focuser (plasma lens):

$$\rho(r,z)=\rho_0(r)+[\rho_f(r)-\rho_0(r)]\,\frac{z}{L}, \tag{11}$$

$$\rho_0=-\frac{I_c}{2\pi cR^2}\left[\frac{\varepsilon^2}{R^2}+\frac{3I}{\beta I_c}\left(1-\frac{r^2}{2R^2}\right)^2\right],$$

$$\rho_f=-\frac{I_c}{2\pi cR^2}\left[\frac{\varepsilon^2}{R^2}+\frac{2I}{\beta I_c}\right]. \tag{12}$$

A plasma lens with a gradually changing particle distribution was considered in Ref. [13]. A simpler way to create a nonlinear potential distribution employs a quadrupole channel with multipole components.

IV. MATCHING OF THE BEAM INTO AN ALTERNATING-GRADIENT FOCUSING CHANNEL WITH HIGHER-ORDER MULTIPOLE COMPONENT

In Ref. [4] it was shown that introducing a duodecapole component in a pure quadrupole alternating-gradient structure results in better matching of the beam with the transport channel, at least at the initial stage of beam transport. Higher-order terms in the potential distribution produce nonlinear components, which can be used to compensate for

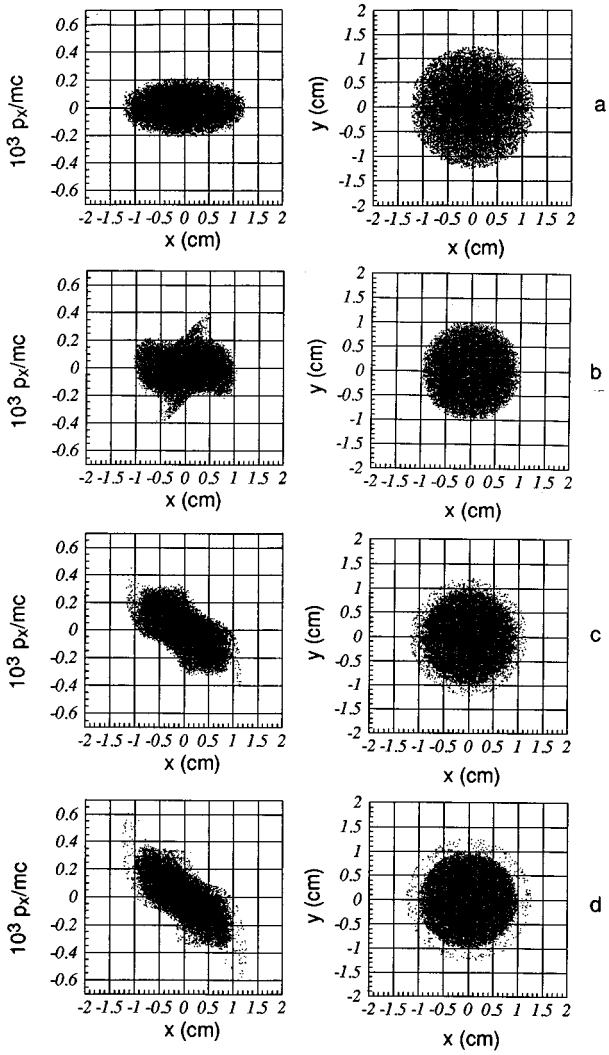

FIG. 6. Halo formation of a circular beam in a pure quadrupole structure with a field gradient $G_2=40$ kV/cm^2: (a) $z=0$, (b) $z=60$ cm, (c) $z=150$ cm, and (d) $z=300$ cm.

nonlinear space charge forces. Let us consider a focusing-defocusing (FD) structure with period $S=2D$, created by a sequence of electrostatic quadrupole lenses of length D. For the magnetic quadrupole channel, the derivations are similar. The structure's potential is given by

$$U(x,y,z)=f(z)\left[\frac{G_2}{2}\,r^2\cos 2\varphi+\frac{G_6}{6}r^6\cos 6\varphi\right], \tag{13}$$

where G_2 is a quadrupole gradient, G_6 is duodecapole component, and the function $f(z)$ represents a z dependence of the potential in alternating-gradient structure

$$f(z)=\begin{cases} 1, & 0<z<\dfrac{S}{2} \\ -1, & \dfrac{S}{2}<z<S. \end{cases} \tag{14}$$

The function $f(z)$ can be expanded as a Fourier series with wave number $k_z=2\pi/S$:

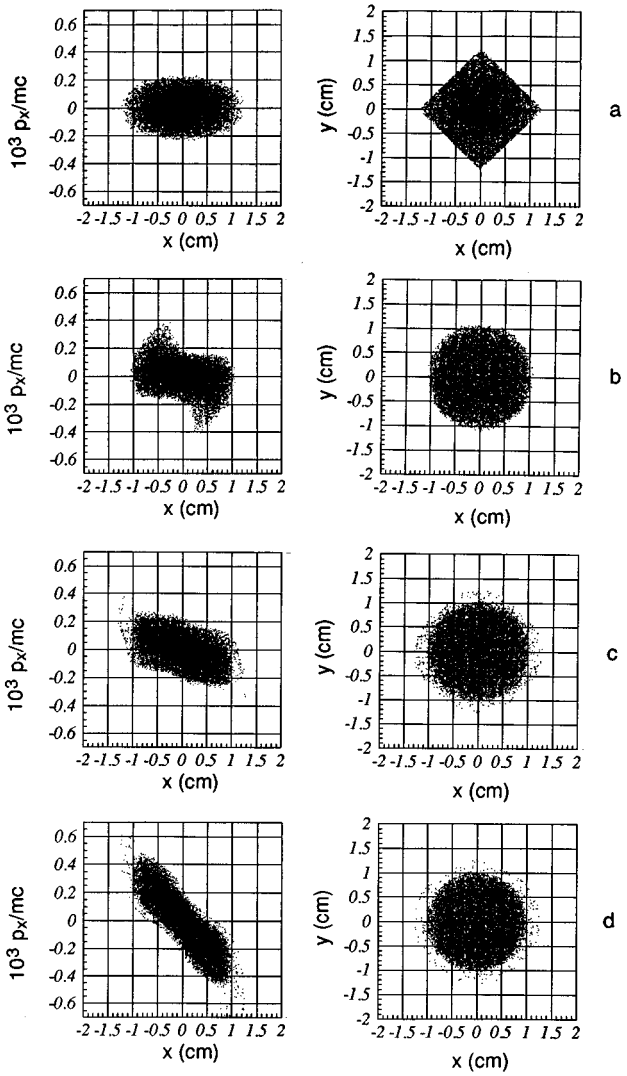

FIG. 7. Halo formation of a square beam in a pure quadrupole structure with field gradient $G_2=40$ kV/cm^2: (a) $z=0$, (b) $z=60$ cm, (c) $z=150$ cm, and (d) $z=300$ cm.

$$f(z)=\frac{4}{\pi}\sin k_z z+\frac{4}{3\pi}\sin 3k_z z+\frac{4}{5\pi}\sin 5k_z z+\cdots+\frac{4}{(2n-1)\pi}\sin(2n-1)k_z z+\cdots . \tag{15}$$

Let us replace the variable z with time $t=z/\beta c$. Particle motion can be considered as fast oscillations in the field

$$\vec{E}(r,\varphi,t)=\sum_{n=1}^{\infty}\vec{E}_{2n-1}(r,\varphi)\sin(2n-1)\omega_0 t, \tag{16}$$

where the frequency $\omega_0=2\pi\beta c/S$ and the field components are

$$\vec{E}_{2n-1}(r,\varphi)=\frac{4}{(2n-1)\pi}[-\vec{i}_r(G_2 r\cos 2\varphi+G_6 r^5\cos 6\varphi)+\vec{i}_\varphi(G_2 r\sin 2\varphi+G_6 r^5\sin 6\varphi)]. \tag{17}$$

The problem of particle motion in a fast oscillating field $\vec{E}(\vec{r},t)=\Sigma_{k=1}^{\infty}\vec{E}_k(\vec{r})\sin\omega_k t$ was analyzed in Refs. [5, 14, 15].

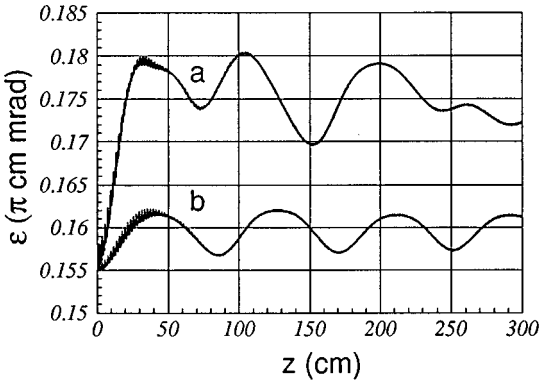

FIG. 8. rms beam emittance growth in a quadrupole field $G_2=40$ kV/cm^2 with an adiabatic decline of the duodecapole component from $G_6=-1$ kV/cm^6 to zero for the distance $0<z<120$ cm followed by a channel with a pure quadrupole field: (a) circular beam and (b) square beam.

Particle trajectories can be represented as a combination of a slow variation of particle position plus small fast oscillations. The oscillating field creates an effective scalar potential

$$U_{\rm eff}(\vec{r})=\frac{q}{4m}\sum_{k=1}^{\infty}\frac{1}{\omega_k^2}E_k^2(\vec{r}), \tag{18}$$

which describes the averaged (slow) motion of particle. For the FD structure the effective potential is

$$U_{\rm eff}=\frac{4}{\pi^2}\frac{qG_2^2}{m\omega_0^2}\left(\sum_{n=1}^{\infty}\frac{1}{(2n-1)^4}\right)[r^2+2\zeta r^6(\cos 2\varphi\cos 6\varphi+\sin 2\varphi\sin 6\varphi)+\zeta^2 r^{10}],$$

$$\zeta=\frac{G_6}{G_2}. \tag{19}$$

The effective potential is an axially nonsymmetric and highly nonlinear function of the radius. The value of the sum in expression (19) is

$$\sum_{n=1}^{\infty}\frac{1}{(2n-1)^4}\approx 1.014\,678 \tag{20}$$

and can be taken as 1. Let us compare the potential (19) for $\varphi=0$ with the required axially symmetric potential (7). Linear focusing parts of the field must be equal:

$$\frac{4}{\pi^2}\frac{qG_2^2}{m\omega_0^2}r^2=\frac{mc^2}{q}\frac{1}{2R^2}\left(\frac{\varepsilon^2}{R^2}+\frac{3I}{I_c\beta}\right)r^2. \tag{21}$$

From Eq. (21) the quadrupole gradient is

$$G_2=\frac{\pi}{2\sqrt{2}}\frac{mc\omega_0}{qR}\sqrt{\frac{\varepsilon^2}{R^2}+\frac{3I}{I_c\beta}}. \tag{22}$$

To define the value of G_6, let us assume that the values of electric fields $E_{\rm ext}=-\partial U_{\rm ext}/\partial r$ and $E_{\rm eff}=-\partial U_{\rm eff}/\partial r$ are equal at the boundary of the beam distribution $r=\sqrt{2}R$. The terms proportional to r^2 vanish due to the adopted condition (21). The remaining terms give the equation

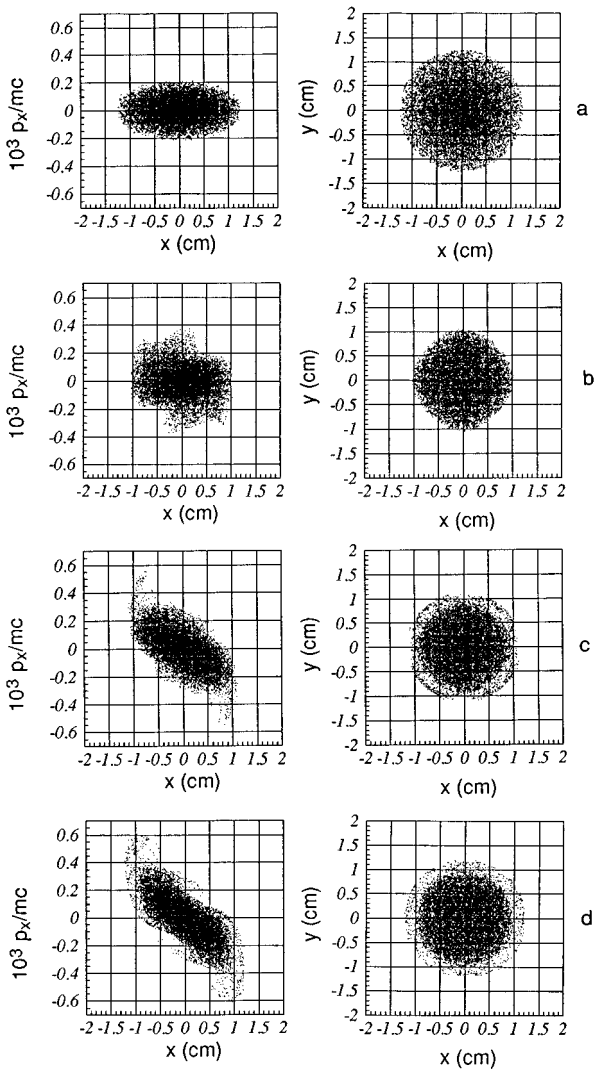

FIG. 9. Halo formation of a circular beam in a quadrupole field $G_2=40$ kV/cm^2 with an adiabatic decline of the duodecapole component from $G_6=-1$ kV/cm^6 to zero for the distance $L=120$ cm: (a) $z=0$, (b) $z=60$ cm, (c) $z=150$ cm, and (d) $z=300$ cm.

$$\frac{8}{\pi^2}\frac{qG_2^2R^5\zeta}{m\omega_0^2}\left[6\left(\frac{r}{R}\right)^5+5\zeta R^4\left(\frac{r}{R}\right)^9\right]\Bigg|_{r/R=\sqrt{2}} =\frac{3}{2}\frac{mc^2}{q}\frac{I}{I_c\beta R}\left[-\left(\frac{r}{R}\right)^3+\frac{1}{6}\left(\frac{r}{R}\right)^5\right]\Bigg|_{r/R=\sqrt{2}}. \tag{23}$$

For usual values of $\zeta R^4 \ll 1$ the second term on the left-hand of Eq. (23) can be neglected. Finally, the duodecapole component is

$$G_6=-\frac{G_2}{R^4}\frac{I}{I_c}\frac{1}{12\beta\left(\dfrac{\varepsilon^2}{R^2}+\dfrac{3I}{I_c\beta}\right)}. \tag{24}$$

For space charge dominated beams, the ''space charge term'' is much larger than the ''emittance term'' $3I/I_c\beta \gg \varepsilon^2/R^2$, which gives

$$G_6=-\frac{1}{36}\frac{G_2}{R^4} \tag{25}$$

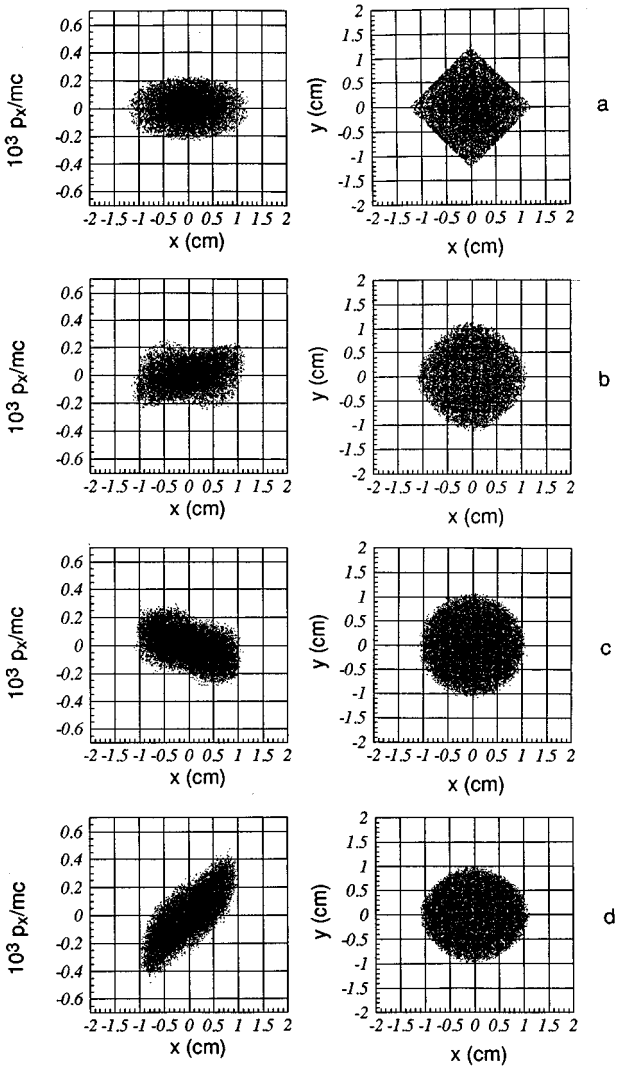

FIG. 10. Adiabatic matching of the beam avoiding halo formation in a quadrupole field $G_2=40$ kV/cm^2 with an adiabatic decline of the duodecapole component from $G_6=-1$ kV/cm^6 to zero for the distance $L=120$ cm: (a) $z=0$, (b) $z=60$ cm, (c) $z=150$ cm, and (d) $z=300$ cm.

or $\zeta R^4=\frac{1}{36}\approx 0.0277$. Note that in every lens the duodecapole component has to be the opposite of the quadrupole component, i.e., the absolute value of the field is reduced in the x and y directions compared to the linear function of the radius.

In Fig. 4 the equipotential lines of the function

$$\Phi=r^2+2\zeta r^6(\cos 2\varphi\ \cos 6\varphi+\sin 2\varphi\ \sin 6\varphi)+\zeta^2 r^{10} \tag{26}$$

are presented. It is seen that for a small radius the lines are close to circles because the quadratic term r^2 is dominant. With a larger radius, the equipotential is close to a 45° skewed square. This suggests that the matched beam should also have the square shape.

Self-consistent computer simulations using particle-in-cell code BEAMPATH were done to verify the matched conditions of the beam, obtained from the above considerations (see Figs. 5–10 and Table II). Parameters of the structure and of the beam with an initial parabolic distribution (1) were cho-

TABLE II. Beam emittance growth in an alternating-gradient focusing channel.

Curve	Beam distribution and focusing channel	Initial emittance (π cm mrad)	Final emittance (π cm mrad)
5*a*	circle beam in a pure quadrupole field	0.155	0.17
5*b*	square beam in a pure quadrupole field	0.155	0.165
8*a*	circle beam in a quadrupole field with a duodecapole component	0.155	0.173
8*b*	square beam in a quadrupole field with a duodecapole component	0.155	0.16

sen as follows: $I=100$ mA, $\varepsilon=0.155$ π cm mrad, $R=1$ cm, $G_2=40$ kV/cm^2, $D=1$ cm, and $G_6=-1$ kV/cm^6. The transverse beam profile in real space was truncated to be a skewed square with the maximum beam size $R_{\max}=2.5\sqrt{\langle x^2\rangle}=1.25R$ [see Fig. 10(a)]. The potential of the structure in simulation was defined by Eq. (13). The value of quadrupole gradient G_2 was kept constant along the channel. The nonlinear component G_6 was adiabatically changed from the value (24) as required by matched conditions to zero, at the distance L:

$$G_6(z)=G_6\left(1-\frac{z}{L}\right). \tag{27}$$

The distance $L=120$ cm was chosen to provide approximately one transverse oscillation of particles. After the nonlinear matcher, $z>L$, the channel was a pure quadrupole and the beam was transported 180 cm further to verify the results of the transformation. A relatively small distance of study was chosen as simulations are time consuming (around 50 h of CPU time on a VAX computer). Meanwhile, even in such a nonadiabatic process, the effect of beam matching into the nonlinear focusing field is clearly visible (Fig. 10).

For comparison, mismatching of a circle beam (Fig. 6) and square beam (Fig. 7) in a pure quadrupole channel as well as mismatching of a circle beam in a nonlinear matcher (Fig. 9) were studied. To make a correct comparison, the same beam with truncated square shape [Fig. 7(a)] as well as a circle beam [Figs. 6(a) and 9(a)] with the same maximum beam size $R_{\max}=2.5\sqrt{\langle x^2\rangle}=1.25$ cm were used in simulations. The beam current $I=100$ mA and initial value of beam emittance $\varepsilon=0.155$ π cm mrad were identical in all cases. Therefore, the total charge of the beam per unit length and phase space density I/ε were the same.

As shown in Figs. 5–7, the beam in a pure quadrupole channel experienced halo formation and emittance growth. Initial values of emittance growth rate are 6×10^{-4} (π cm mrad)/cm for a circular beam and 4×10^{-4} (π cm mrad)/cm for a square beam. After 30 lenses, which correspond to one-quarter of a transverse oscillation, the beam emittance achieved the value 0.176 π cm mrad for a circular beam and 0.168 π cm mrad for an initially square beam shape. Finally, a beam halo was formed and the rms beam emittance became stable with values of 0.17 π cm mrad for a circular beam and 0.165 π cm mrad for an initially square beam shape.

In Figs. 8–10 results of the beam dynamics study in a nonlinear matcher are presented. The introduction of a duodecapole component in a pure quadrupole channel is a necessary but not sufficient condition to provide beam matching. A nonuniform beam with a circular cross section remains mismatched in a nonlinear alternating-gradient field. In Figs. 8(a) and 9 emittance growth and halo formation of such a beam in a nonlinear matcher are presented. The initial emittance growth rate is 8×10^{-4} π cm mrad/cm and the final value of beam emittance is 0.173 π cm mrad. To avoid halo formation, the nonuniform beam must be truncated in real space with a square shape, as shown in Fig. 10.

For the square beam in a nonlinear matcher, the initial value of emittance growth rate is 2×10^{-4} (π cm mrad)/cm [Fig. 8(b)], which is substantially smaller than in mismatched beam transport. The final value of beam emittance is 0.16 π cm mrad, which indicates better matching conditions than in previous cases presented in Figs. 6, 7, and 9. The beam profile in real space is transformed from a square to a circular shape (Fig. 10) and follows the adiabatic change of the effective potential. The final beam emittance and beam profile are matched with the linear focusing channel without halo and phase-space distortion.

The above consideration demonstrates that two conditions are essential to keep emittance growth down: (i) introduction of a sixth-order component in a pure quadrupole alternating-gradient structure and (ii) square truncation of a nonuniform distribution in real space. As shown in Fig. 10(a), the truncation does not disturb the shape of beam emittance at the phase plane $x-p_x$. After nonlinear matcher the beam emittance is close to the initial unperturbed ellipse without a halo in phase space, which facilitates the subsequent matching of the beam with a linear focusing channel. Since nonlinear space charge effects are pronounced at low beam energy, square beam truncation can be performed during extraction from the particle source with a square extraction hole.

V. SCALING PARAMETERS

The above relationships allow us to introduce scaling parameters that can be used for possible simulation of a high-current, high-energy beam by a small-scaled beam. Let us introduce dimensionless beam emittance η and beam current j, which must be the same for scaling beams

$$\eta=\frac{\varepsilon}{R}, \quad j=\frac{I}{I_c\beta}. \tag{28}$$

Required values for the quadrupole gradient, duodecapole component, and period of FD structure are scaled as

$$g_2=\frac{qG_2R^2}{mc^2\beta}\,\theta, \quad g_6=\frac{qG_6R^6}{mc^2\beta}\,\theta, \quad \theta=\frac{S}{R}. \tag{29}$$

While the scaled period of the structure θ is the same for scaling beams, the number of lenses is different. Let us consider the equation of particle motion in an effective potential (19):

$$\frac{d^2x}{d\upsilon^2}=-\frac{q}{m}\left(\frac{S}{\beta c}\right)^2\frac{\partial U_{\rm eff}}{\partial x}, \quad \upsilon=\frac{z}{S}. \tag{30}$$

After some algebra, one gets the frequency of smoothed transverse linear oscillations μ_0:

$$\frac{d^2x}{d\upsilon^2}=-\mu_0^2(x+6\zeta x^5+5\zeta^2x^9), \quad \mu_0=\frac{\sqrt{2}}{\pi^2}\frac{S^2G_2q}{mc^2\beta^2}. \tag{31}$$

The value of μ_0 is a phase shift of transverse oscillations per period of structure S in an effective field of the structure (19). Taking into account the expression for quadrupole gradient G_2 (22), the value of μ_0 is scaled as

$$\mu_0\sim\frac{\theta}{\beta}. \tag{32}$$

This means that for the same values of dimensionless period of the structure θ, the value of μ_0 is inversely proportional to velocity of particles. To obtain the same total phase shift of transverse oscillations for a beam with higher energy, a larger number of lenses is required. Using the linear part of space charge potential of the beam (4), the depressed value of phase advance per period for a space charge dominated regime is

$$\mu=\frac{\mu_0}{1+3\,\dfrac{j}{\eta^2}}. \tag{33}$$

Introducing these scaling parameters allows us to simulate a heavy ion, high current beam by a light ion beam with smaller energy and smaller current.

VI. CONCLUSION

The adiabatic change of a nonlinear focusing field along a beam guiding structure results in the gradual transformation of an initially nonlinear beam distribution into a distribution matched with the linear focusing channel. This avoids otherwise substantial emittance growth during the stage of beam transport. Two cases of a nonlinear focusing field were considered: a plasma lens and an alternating gradient focusing structure with a duodecapole component. In the latter case, the beam shape in real space has to be close to square, which corresponds to the matched conditions of the beam with an averaged nonlinear focusing field. The suggested scheme enables us to transform a laboratory beam with a nonlinear distribution function into a beam that is matched with the linear focusing without halo formation. After transformation, the beam can be transported (accelerated) in a conventional structure with a linear focusing field.

ACKNOWLEDGMENTS

The author is indebted to T. Ray, B. McGinnis, and J. Schubert for their careful reading of the manuscript and many suggestions for its improvement.

[1] R. C. Arnold, Nature **276**, 19 (1978).
[2] R. A. Jameson, G. P. Lawrence, and S. O. Schriber, in *Proceedings of the Third European Particle Accelerator Conference, Berlin, 1992*, edited by H. Henke, H. Homeyer, and Ch. Petit-Jean-Genaz (Editions Frontieres, Paris, 1992), p. 230.
[3] Y. Batygin, in *Proceedings of the 17th International Linac Conference*, edited by K. Takata, Y. Yamazaki, and K. Nakahara (National Laboratory for High Energy Physics, Tsukuba, 1994), p. 487.
[4] Y. Batygin, Phys. Rev. E **53**, 5358 (1996).
[5] L. Landau and E. Lifshitz, *Mechanics* (Pergamon, New York, 1975).
[6] I. M. Kapchinsky, *Theory of Resonance Linear Accelerators* (Atomizdat, Moscow, 1966).
[7] J. D. Lawson, *The Physics of Charged-Particle Beams* (Clarendon, Oxford, 1977).
[8] P. M. Lapostolle, IEEE Trans. Nucl. Sci. **NS-18**, 1101 (1971).
[9] J. Struckmeier and I. Hofmann, Part. Accel. **39**, 219 (1992).
[10] M. Reiser, *Theory and Design of Charged Particle Beams* (Wiley, New York, 1994).
[11] Y. Batygin, in *Proceedings of the Third European Particle Accelerator Conference, Berlin, 1992* (Ref. [2]), p. 822.
[12] R. W. Hockney and J. W. Eastwood, *Computer Simulation Using Particles* (McGraw-Hill, New York, 1981).
[13] P. Chen, K. Oide, A. M. Sessler, and S. S. Yu, Phys. Rev. Lett. **64**, 1231 (1990).
[14] G. M. Zaslavsky and R. Z. Sagdeev, *Introduction to Nonlinear Physics* (Nauka, Moscow, 1988).
[15] A. V. Gaponov and M. A. Miller, Zh. Eksp. Teor. Fiz. **34**, 242 (1958).